Channel-containing structure built of 3D sodium nitrate coordination polymer

A. Trzesowska[a]; R. Kruszynski[a]

[a] Department of X-Ray Crystallography and Crystal Chemistry, Institute of General and Ecological Chemistry, Technical University of Lodz, Zeromskiego 116, 90-924 Lodz, Poland

PLEASE SCROLL DOWN FOR ARTICLE

Taylor & Francis
Taylor & Francis Group

Channel-containing structure built of 3D sodium nitrate coordination polymer

A. TRZESOWSKA* and R. KRUSZYNSKI

Department of X-Ray Crystallography and Crystal Chemistry, Institute of General and Ecological Chemistry, Technical University of Lodz, Zeromskiego 116, 90-924 Lodz, Poland

The three-dimensional channel structure of catena-((μ_3-hexamethylenetetraamine)-*tris*-(μ_3-nitrato)-tri-sodium), $[(NaNO_3)_3 \cdot (CH_2)_6N_4]_n$, is presented. The sodium is seven coordinate with a distorted capped trigonal prism geometry. During heating the hexamethylenetetraamine can be removed from the compound. The principal volatile thermal decomposition and fragmentation products correspond to: C^+, CO_2^+, NO^+, N_2O^+.

Keywords: Sodium coordination polymer; Channel structure; Hexamethylenetetraamine; TG-MS system

1. Introduction

Design and synthesis of metal–organic and mixed metal–inorganic/organic host microporous coordination polymers are of interest because of their potential application as functional materials in the areas of catalysis, ion-exchange and separation [1, 2]. Framework structures enclose channels or cavities and may act as hosts for various guest species [3–5]. The flexibility of the metal–organic framework is used in molecular recognition and selective guest inclusion. The only limitation is their lower thermal stability, restricted by the strength of the metal–ligand bonds [6, 7].

The benefits of inorganic host frameworks are robustness and high thermal stability enabling removal of guest species without collapsing the structure. These materials offer excellent separation properties by shape-selective adsorption or molecular sieving [8]; the number of such analogues of zeolites is still growing. The present study is aimed at the synthesis, structural, spectroscopic and thermal characterization of a metal–inorganic guest-host coordination polymer, $[(NaNO_3)_3 \cdot (CH_2)_6N_4]_n$. The framework structure is built by sodium nitrate, whereas the hexamethylenetetraamine molecules (hmt), the smallest member of tricyclic tetraamines so-called cage-adamanzanes [9], are encapsulated within the channels from which they cannot escape, as they are

---

*Corresponding author. Tel.: +48-42-631-31-37. Fax: +48-42-631-31-03. Email: agata.trzesowska@p.lodz.pl

coordinately bonded to sodium ions. Nevertheless, the molecules of hmt can be easily removed during heating.

2. Experimental

2.1. Synthesis of $[(NaNO_3)_3 \cdot (CH_2)_6N_4]_n$

The compound was obtained by reaction of sodium nitrate (0.255 g, 3 mmol) dissolved in $10 \, cm^3 \, H_2O$ with cooled saturated aqueous solutions of hexamethylenetetraamine (0.14 g, 1 mmol). The solution was stirred at room temperature and left to crystallize at 278 K. After several days, colorless crystals formed. IR (KBr, cm^{-1}): 2955m (νCH_2), 2872m (νCH_2), 1485s (νNO_3), 1458m (νCH_2), 1374m (νCH_2), 1290m (νNO_3), 1240m (νCN), 1041s (νCN and/or νNO_3), 1009s (νCN), 983s (νCN), 958s (νCN), 817s (νCH_2 and/or νNO_3), 671m (νCN), 513w (νCN), 501w (νCN).

2.2. X-ray crystallography

A rectangle prism $(0.067 \times 0.068 \times 0.070 \, mm^3)$ was mounted on a KM-4-CCD automatic diffractometer equipped with a CCD detector and used for data collection. X-ray intensity data were collected with graphite monochromated Mo-Kα radiation ($\lambda = 0.71073 \, \text{Å}$) at 293.0(2) K with ω scan mode. A 7 s exposure time was used and all reflections inside the Ewald sphere were collected up to $2\theta = 62.88°$ with scan width $0.5°$. The unit cell parameters were determined from the 5429 strongest reflections. The crystal used for data collection did not change appearance. Lorentz, polarization and numerical absorption [10] corrections were applied. The structure was solved by direct methods and subsequently completed by difference Fourier recycling. All non-hydrogen atoms were refined anisotropically using full matrix, least-squares on F^2. The hydrogen atoms of hexamethylenetetraamine were placed in idealized positions and refined with a riding model. SHELXS97 [11], SHELXL97 [12] and SHELXTL [13] programs were used for all the calculations. Atomic scattering factors were those incorporated in the computer programs. Details concerning crystal data and refinement are summarized in table 1 and selected bond lengths and angles are given in table 2.

2.3. Physical measurements

The IR spectrum (400–4000 cm^{-1}) was recorded with a Shimadzu DR-8011 spectrophotometer. Thermal analysis was carried out in a TG/DTA-SETSYS-16/18 thermoanalyzer coupled with a ThermoStar (Balzers) mass spectrometer. The sample (6.45 mg) was heated in corundum crucible up to 1000°C at the heating rate 10°C min^{-1} in air. The products of decomposition were calculated from the TG curve. The temperature ranges were determined by means of the thermoanalyzer Data Processing Module [14]. The coupled TG-MS system was used to analyze the principal volatile thermal decomposition and fragmentation products. Elemental analysis (C, H) was carried out with a EuroVector 3018 analyzer. The samples were

Table 1.   Crystal data and refinement for $[(NaNO_3)_3 \cdot (CH_2)_6N_4]_n$.

Empirical formula	$C_6H_{12}O_9N_7Na_3$
Formula weight	395.20
Crystal system	Trigonal
Space group	$R3c$
Unit cell dimensions (Å)	
a	14.8056(7)
c	12.1621(12)
Volume (Å^3)	2308.8(3)
Z	6
Absorption coefficient (mm^{-1})	0.222
$F(000)$	1212
θ range for data collection (°)	3.71–31.44
Index ranges	$-19 \leq h \leq 20, -21 \leq k \leq 18, -17 \leq l \leq 15$
Goodness-of-fit on F^2	1.001
Final R indices $[I > 2\sigma(I)]$	$R_1 = 0.0258, wR_2 = 0.0765$
R indices (all data)	$R_1 = 0.0268, wR_2 = 0.0777$
Largest difference peak and hole (e Å^{-3})	0.191 and -0.143

Table 2.   The selected bond lengths [Å] and angles [°] for
$[(NaNO_3)_3 \cdot (CH_2)_6N_4]_n$.

Na(1)–O(1)	2.6219(15)
Na(1)–O(2)	2.4455(13)
Na(1)–O(2A)^i	2.4969(13)
Na(1)–O(3A)^i	2.4388(12)
Na(1)–O(1B)^{ii}	2.6147(15)
Na(1)–O(3B)^{ii}	2.3926(12)
Na(1)–N(1)	2.5485(11)
N(1)–C(1)	1.4774(14)
N(1)–C(2)	1.4836(16)
C(2)–N(2)	1.4737(14)
C(1)–N(1)–C(2)	107.74(9)
N(1)–C(2)–N(2)	112.31(10)
H(2A)–C(2)–H(2B)	107.86
N(1)–C(2)–N(2)–C(2D)^{iii}	58.77(12)
H(2A)–C(2)–N(1)–C(1)	179.52
H(2B)–C(2)–N(1)–C(1)	62.82

Symmetry codes: (i) $-x+y-4/3, -x-2/3; z+1/3$, (ii) $-x+y-5/3, y-1/3$, $z+1/6$; (iii) $-x+y-1, -x-1, z$.

milled in the planetary ball corundum mill for 5 min, and next the X-ray powder diffraction patterns were measured in reflection mode on an XPert PRO X-ray powder diffraction system equipped with a Bragg-Brentano PW 3050/65 high resolution goniometer and PW 3011/20 proportional point detector using Cu-Kα_1 radiation. The patterns were measured at 291.0(2) K in the range 5–50° with the narrowest beam attenuator. The 60 seconds per 0.002° step procedure was used. The samples were sprinkled onto the sample holders using a small sieve to avoid a preferred orientation. The thickness of the samples was no more than 0.1 mm. During the measurements each specimen was spun in the specimen plane to improve particle statistics.
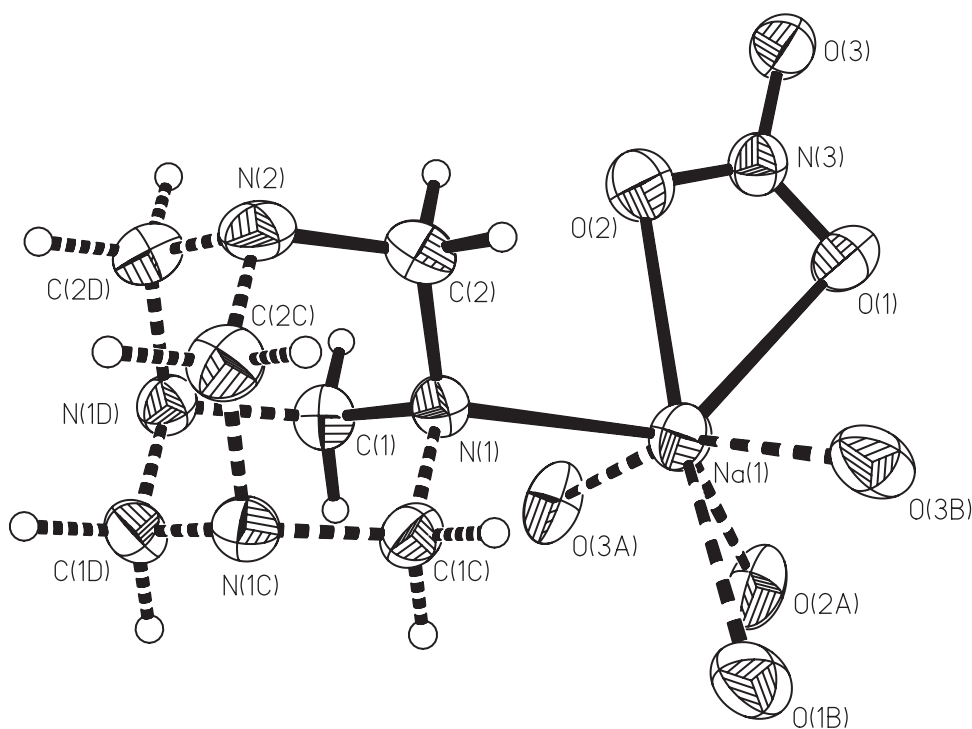
Figure 1. The molecular structure of the sodium coordination polymer. Solid lines indicate the content of the asymmetric unit. The displacement ellipsoids are drawn at 50% probability.

3. Results and discussion

3.1. *The structure description*

The sodium ion is seven-coordinate by oxygen atoms of bidentate nitrate groups and nitrogen atom of hexamethylenetetraamine; the cell asymmetric unit is presented in figure 1. The coordination polyhedron can be described as a distorted capped trigonal prism (figure 2). The Na–O bond lengths vary from 2.3926(12) to 2.6219(15) Å, whereas the Na–N (hmt) distance is 2.5485(11) Å. The C–N bond lengths of the hmt molecule lie in the range 1.4737(14)–1.4836(16) Å and are comparable to C–N bond lengths found by Terpstra and Craven [15].

Only one nitrate group is unsymmetrically bound to the sodium [16]. The difference between the Na–O bond lengths of this nitrate group is 0.221 Å. The planarity of the nitrate group is not strictly preserved but the three O–N–O angles do not deviate significantly from 120°. The terminal N–O bonds are slightly lengthened (average distance 1.247 Å) and the Na–O bonds are shortened (average distance 2.502 Å) in comparison with the bond lengths of glycine sodium nitrate (1.241 and 2.653 Å, respectively) [17], in which three nitrate ions are asymmetrically bonded to the eight-coordinate Na. The difference of nitrate bonding in these two coordination polymers appears to be a function of electronic distribution at sodium ion or the position of organic ligand toward coordinated oxygen atoms of bidentate nitrogen groups.
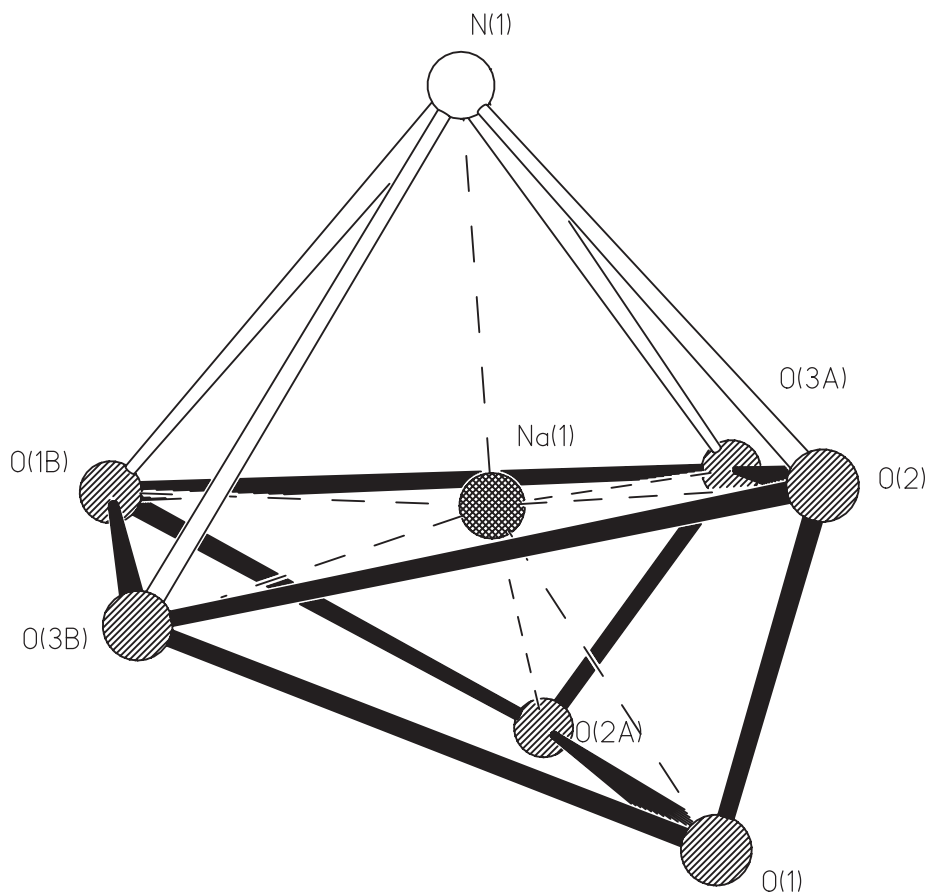
Figure 2.   The coordination polyhedron around the sodium atom.

The three nitrogens atoms of the nitrate ions and the nitrogen atom of hexamethylenetetraamine form a distorted tetrahedron around the sodium ion. The dihedral angles formed by the three weighted least-square planes calculated through the sodium-nitrate moieties are 70.85 (6)° (between nitrate group and nitrate group generated by $-x+y-5/3$, $y-1/3$, $z+1/6$ symmetry transformation), 73.37 (6)° (between nitrate group generated by $-x+y-4/3$, $-x-2/3$, $z+1/3$ symmetry transformation and nitrate group generated by $-x+y-5/3$, $y-1/3$, $z+1/6$ symmetry transformation) and 87.88 (6)° (between nitrate group and nitrate group generated by $-x+y-4/3$, $-x-2/3$, $z+1/3$ symmetry transformation). Atoms O(2B), O(1A) and O(3) have the largest deviations from the above mentioned planes and they are out of plane by -0.1037, -0.0988 and 0.0396 Å, respectively, which is in agreement with the bonding mode of two oxygen atoms of bidentate nitrate groups.

The sodium and nitrate ions form a 3D channel structure along the *c*-axis with hmt molecules placed in the center (figure 3). Hmt is a trifunctional ligand bonded to sodium ions (figure 3). The channel diameter is about 9 Å. All hmt molecules are shifted about 6 Å to each other along the *c*-axis. A similar three-dimensional framework based on metal ions bound to hmt and nitrate anions can be found in a coordination polymer of empirical formula $[Ag_2(hmt)(NO_3)_2]_n$ [18]. However, the anion bridges form a helical
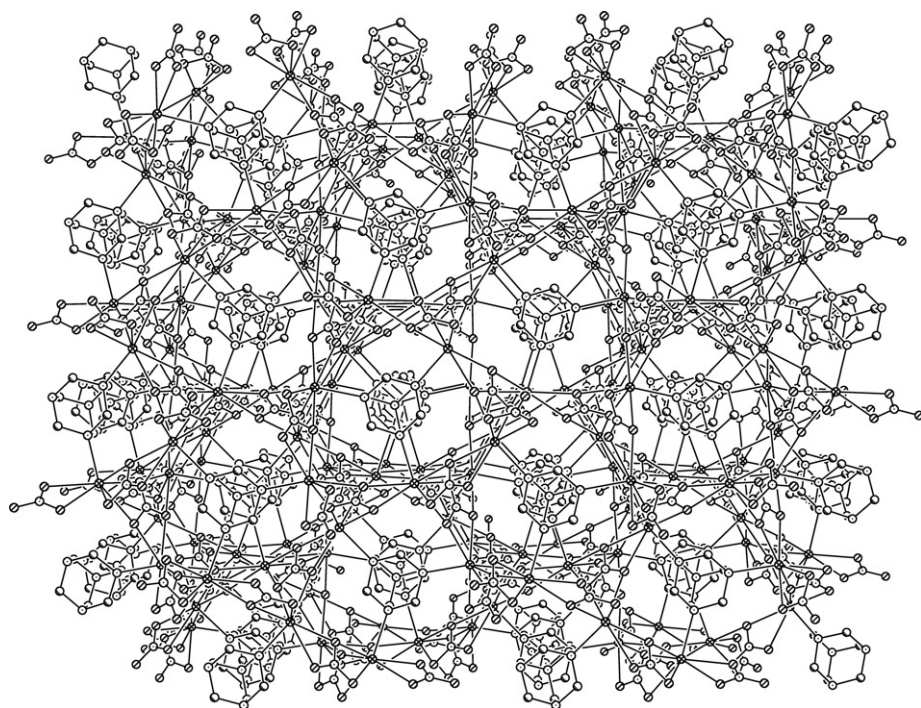
Figure 3. A packing view along the *c* direction.

cylinder structure motif in comparison with the channel framework structure observed in $[(NaNO_3)_3(hmt)]_n$. In the compound under study, hmt acts as a guest molecule (figure 4 [19]). Generally hmt forms metal–hmt frameworks [20–26]. No hydrogen bonds were observed between the guest and the host molecules.

3.2. *IR spectrum*

The vibrational frequencies of methylene (hmt) and nitrate ions partially overlap making it difficult to establish the bonding of nitrates, e.g. the band at $817 \, cm^{-1}$ can be associated with C–H rocking vibration or out-of-plane deformation of nitrate group. The strong splitting of the normally degenerate asymmetric stretching band of nitrate ions to a doublet at $1485 \, cm^{-1}$ and $1290 \, cm^{-1}$ indicates they are bidentate chelating ligands [27]. The difference between these vibrational frequencies of symmetric stretching bands is $195 \, cm^{-1}$, indicating that Na–O (nitrate) bonds are relatively strong. The split bands of the CN bending and stretching vibrations at $511 \, cm^{-1}$ and $1009 \, cm^{-1}$ are attributed to forming bonds between hmt and sodium ions [28], in agreement with the structural analysis discussed above.

3.3. *Thermal behavior*

The compound is stable to $110°C$ (figure 5). Upon heating to $1000°C$ in the air, three successive mass loss intervals were observed. The first endothermic step, occurring to
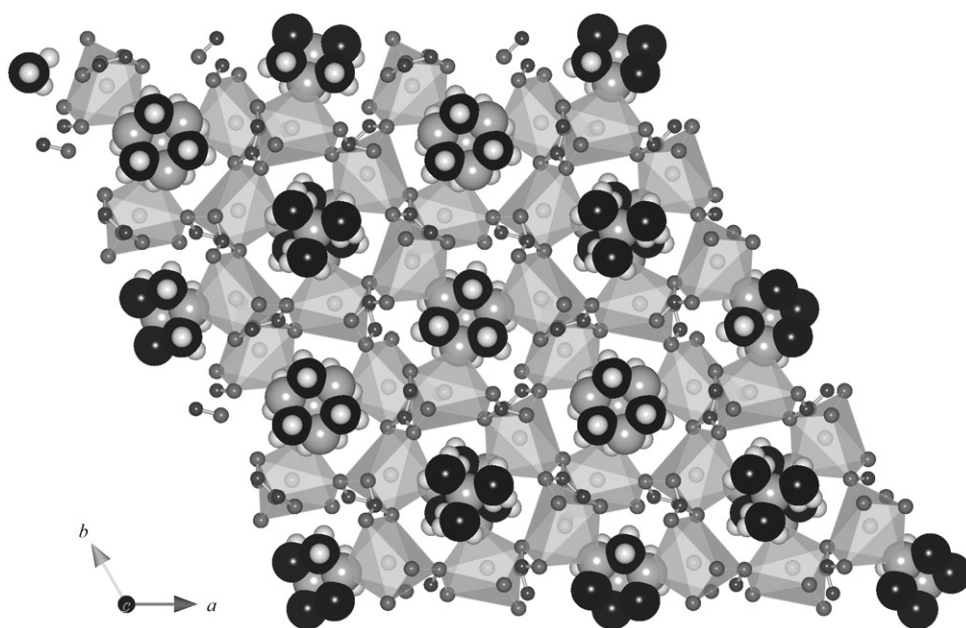
Figure 4.   The network of coordination polymer, Na ion coordination sphere in polyhedral mode and hmt molecules in space-filling mode.

the temperature 290°C, corresponds to weight loss of 34.7% and is attributed to the loss of the hmt (theoretical value is 35.4%). The observation that hmt is easily lost at this temperature range is consistent with elemental analysis in which carbon was not detected. The XRPD pattern shows that the decomposition leads to an unidentified crystalline phase (figure 6), which is definitely not a known structure of sodium nitrate [29]. The DTA and DTG curves indicate a two-stage removal process, but the individual steps on the TG curve are impossible to distinguish. However, the mass spectrum of the thermal decomposition of sodium coordination polymer does not show any ion current signals. According to Gusev *et al.* [30] at atmospheric pressure hmt sublimes at 263°C. Owing to the construction of the thermoanalyzer-mass spectrometer system, in which the evolved gases are removed from the furnace chamber and carried in a stream of air flowing at a constant rate and temperature to the detector, after sublimation the hexamethylenetetraamine may crystallize inside the system and decompose at higher temperatures. This is the reason why the gaseous products of hmt decomposition are recorded between 300°C and 1000°C, despite the fact that mass loss indicates total removal of hmt at 260°C. Pure hexamethylenetetraamine decomposes up to 270°C, while the gaseous products are detected up to 650°C. The hmt decomposes gradually with releasing C^+ ($m/z = 12$), NO^+ ($m/z = 30$) and CO_2^+, N_2O or $N(CH_3)_2$ ($m/z = 44$), which may have been formed during ammonia or methylamine oxidation. Forming of other typical hmt decomposition products, such as N_2, NH_3, was not observed. The succeeding two stages are also endothermic. However, the second step (from 290 to 480°C) occurs almost without mass loss (0.5%), corresponding to melting of sodium nitrate (peak at 310°C on the DTG curve) and destruction of its structure. The XRPD pattern of sample heated to 350°C (above the melting point of the
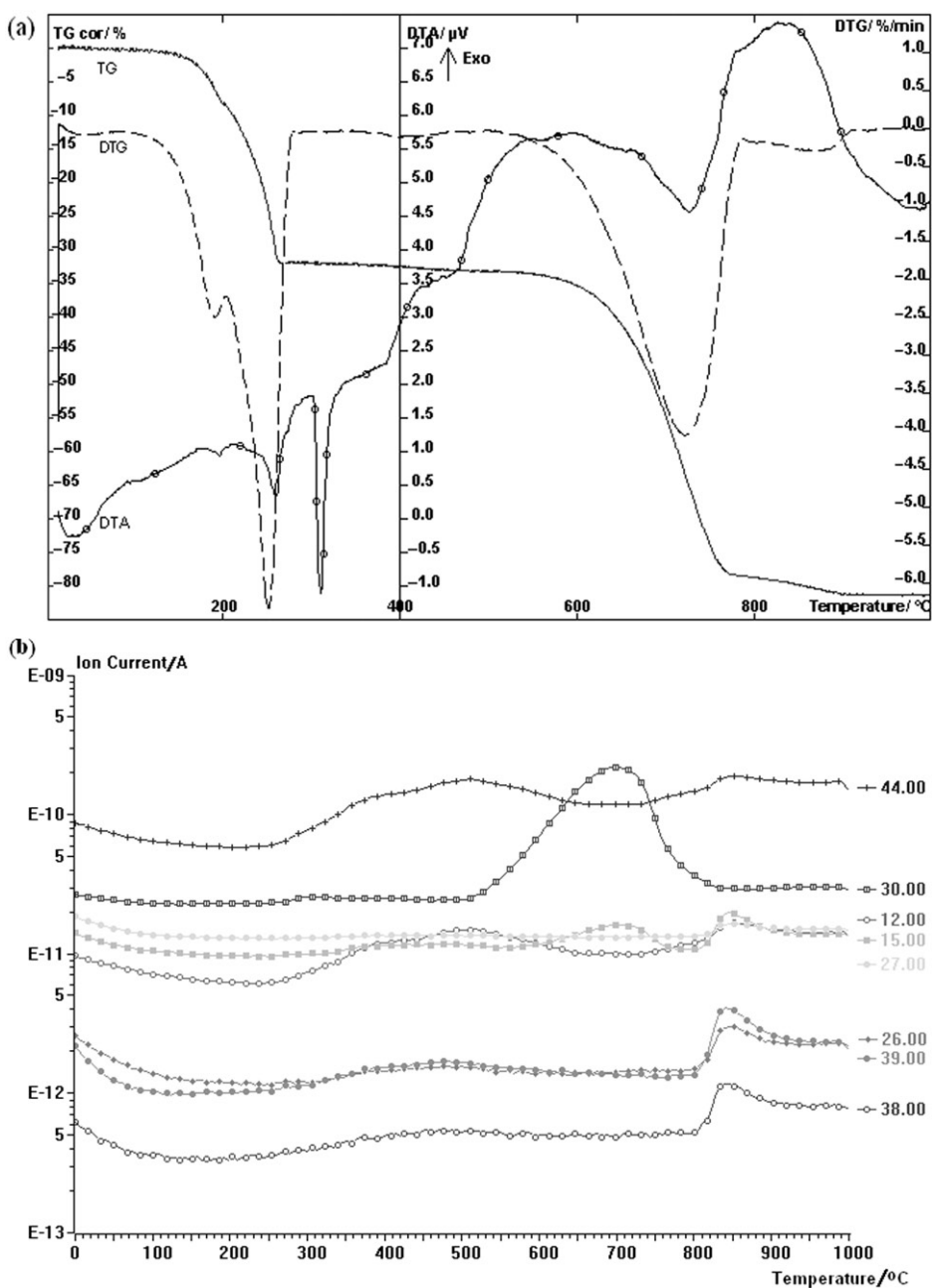
Figure 5.   (a) The TG, DTG and DTA curves. (b) The gaseous products of the thermal decomposition of sodium complex.

unidentified phase) and cooled to room temperature shows only one phase, $NaNO_3$ [29], indicating the unidentified phase is a different form of $NaNO_3$. The next step of decomposition (480–780°C) is characterized by strong peaks on the DTA (726°C), DTG (720°C) curves and the biggest mass loss (43.1%). The main volatile
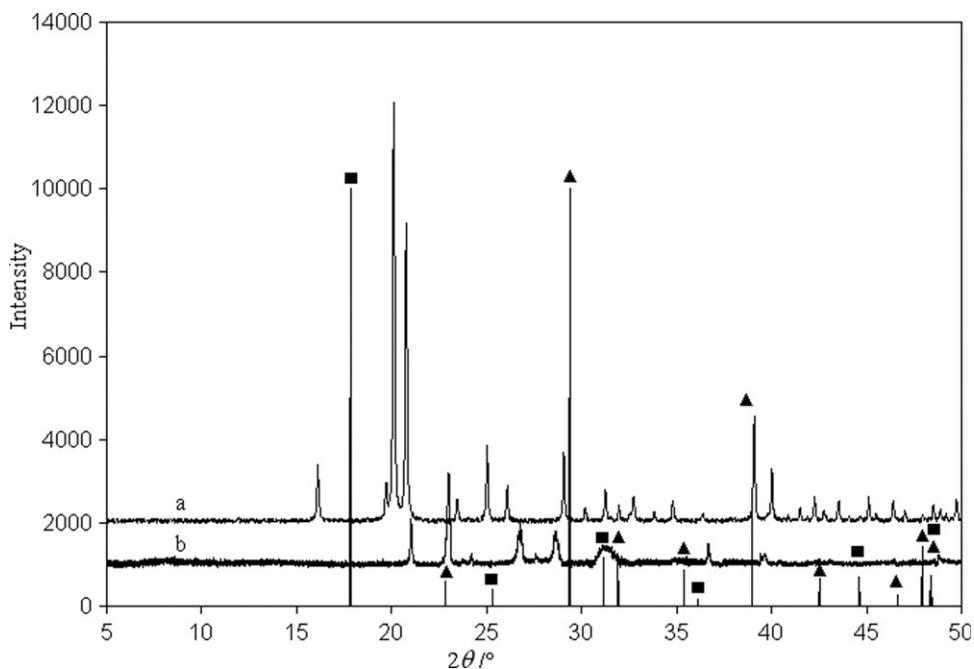
Figure 6. XRPD patterns of a: sodium nitrate complex with hmt, b: unidentified phase obtained by the thermal decomposition of coordination polymer, triangle: pure sodium nitrate (simulated on the basis of crystal structure [29]), square: hmt (simulated on the basis of crystal structure [15]).

products include nitrogen oxide ($m/z = 30$), as a result of nitrate group decomposition as well as NH^+ ($m/z = 15$), as a result of hmt decomposition. In previous work [31–33] this oxide was reported as a product of thermal decomposition of transition metal hydrated nitrates. The MS spectrum does not show the presence of other typical nitrate decomposition products such as NO_2 or HNO_3. Even if NO_2 is formed, the existence of NO instead of NO_2 may be observed due to fragmentation of NO_2 to NO or due to the following reaction: $NO_2 + O \rightarrow NO + O_2$. The last decomposition step occurs in the range 780–910°C and is accompanied by a broad exothermic peak (847°C) on the DTA curve and the small mass loss of 3%. This step is related with decomposition of nitrate ions ($m/z = 44$ corresponds to N_2O). The signal with $m/z = 26, 27, 38, 39$ can be attributed to CN^+, HCN^+, C_2N^+, HC_2N^+, from the hmt decomposition. Total mass loss is equal to 81.3%. The final product of complex decomposition is Na_2O.

4. Conclusions

The new 3D robust inorganic coordination polymer, in which the hmt is a guest molecule, has been synthesized and characterized. The Na–N coordination bonds can be broken and neutral hmt molecules can be totally removed from the compound by heating the compound to 290°C. The structure of inorganic framework above this temperature is different than known structures of $NaNO_3$ salt, suggesting that part of the channel structure may be retained.

Supplementary material

Crystallographic data for the structure have been deposited with the Cambridge Crystallographic Data Centre, CCDC No. 266846. Copies of the data can be obtained free of charge on application to The Director, CCDC, 12 Union Road, Cambridge CB2 1EZ, UK (Fax: +44(1223)336-033; Email for inquiry: fileserv@ccdc.cam.ac.uk; Email for deposition: deposit@ccdc.cam.ac.uk).

Acknowledgements

References

[1] A.M. Goforth, K. Gerth, M.D. Smith, S. Shotwell, U.H.F. Bunz, H.-C. zur Loye. *Solid State Sci.*, **7**, 1083 (2005).
[2] Y. Cui, H.L. Ngo, W. Lin. *Inorg. Chem.*, **41**, 5940 (2002).
[3] W.J. Belcher, C.A. Longstaff, M.R. Neckenig, J.W. Steed. *Chem. Commun.*, 1602 (2002).
[4] S. Noro, S. Kitagawa, M. Yamashitac, T. Wadab. *Chem. Commun.*, 222 (2002).
[5] J.Y. Lu, A.M. Babb. *Chem. Commun.*, 1346 (2003).
[6] M. Du, X.-J. Zhao, Y. Wang. *Dalton Trans.*, 2065 (2004).
[7] A. Dimos, D. Tsaousis, A. Michaelides, S. Skoulika, S. Golhen, L. Ouahab, C. Didierjean, A. Aubry. *Chem. Mater.*, **14**, 2616 (2002).
[8] M.W. Anderson, O. Terasaki, T. Ohsuna, A. Philippou, S.P. MacKay, A. Ferreira, J. Rocha, S. Lidin. *Nature*, **367**, 347 (1994).
[9] J. Springborg. *Dalton Trans.*, 1653 (2003).
[10] X-RED. *Version 1.18. STOE & Cie GmbH*, Darmstadt, Germany (1999).
[11] G.M. Sheldrick. *Acta Cryst.*, **A46**, 467 (1990).
[12] G.M. Sheldrick. *SHELXL97 Program for the Solution and Refinement of Crystal Structures*, University of Göttingen, Germany (1997).
[13] G.M. Sheldrick. *SHELXTL: Release 4.1 for Siemens Crystallographic Research Systems*, Madison, Wisconsin, USA (1990).
[14] Data processing Module, Copyright © 1994–1998 SETARAM – FRANCE; Version 1.4.
[15] M. Terpstra, M. Craven. *Acta Cryst.*, **A49**, 685 (1993).
[16] C.C. Addison, N. Logan, S.C. Wallwork, C.D. Garner. *Q. Rev. Chem. Soc.*, **25**, 289 (1971).
[17] R.V. Krishnakumar, M. Subha Nandhini, S. Natarajan, K. Sivakumar, B. Varghese. *Acta Cryst.*, **C57**, 1149 (2001).
[18] W.-M. Bu, L. Ye, Y.-G. Fan. *Chem. Lett.*, **29**, 152 (2000).
[19] F. Izumi, R.A. Dilanian. *Commission on Powder Diffr., IUCr Newslett.*, **32**, 59 (2005).
[20] S.-L. Zheng, M.-L. Tong, H.-L. Zhu, X.-M. Chen. *New J. Chem.*, **25**, 1425 (2001).
[21] Q. Liu, Y. Li, H. Liu, F. Wang, Z. Xu. *J. Mol. Chem.*, **733**, 25 (2005).
[22] L. Carlucci, G. Ciani, D.M. Proserpio, A. Sironi. *J. Am. Chem. Soc.*, **117**, 12861 (1995).
[23] W.-M. Bu, L. Ye, Y.-G. Fan. *Inorg. Chem. Commun.*, **3**, 194 (2000).
[24] L. Carlucci, G. Ciani, D.M. Proserpio, S. Rizzato. *J. Solid State Chem.*, **152**, 211 (2000).
[25] S.-L. Zheng, M.-L. Tong, S.-D. Tan, Y. Wang, J.-X. Shi, Y.-X. Tong, H.K. Lee, X.-M. Chen. *Organometallics*, **20**, 5319 (2001).
[26] S.-L. Zheng, M.-L. Tong, X.-M. Chen. *Coord. Chem. Rev.*, **246**, 185 (2003).
[27] N.F. Curtis, Y.M. Curtis. *Inorg. Chem.*, **4**, 804 (1965).

[28] Y. Zhang, J. Li, M. Nishiura, T. Imamoto. *J. Mol. Chem.*, **523**, 257 (2000).
[29] W. Gonschorek, W.W. Schmahl, H. Weitzel, G. Miehe, H. Fuess. *Z. Kristallogr.*, **210**, 849 (1995).
[30] E.A. Gusev, S.V. Dalidovich, L.I. Krasovskaya. *Thermochim. Acta*, **93**, 21 (1985).
[31] A. Małecki, R. Gajerski, S. Łabuś, B. Prochowska-Klisch, K.T. Wojciechowski. *J. Therm. Anal. Calorim.*, **60**, 17 (2000).
[32] A. Małecki, B. Małecka, R. Gajerski, S. Łabuś. *J. Therm. Anal. Calorim.*, **72**, 135 (2003).
[33] K.T. Wojciechowski, A. Małecki. *Thermochim. Acta*, **331**, 73 (1999).